Unique Transcriptome, Pathways, and Networks in the Human Endometrial Fibroblast Response to Progesterone in Endometriosis 1

Authors: Aghajanova, L., Tatsumi, K., Horcajadas, J.A., Zamah, A.M., Esteban, F.J., et al.

Source: Biology of Reproduction, 84(4) : 801-815

Published By: Society for the Study of Reproduction

URL: https://doi.org/10.1095/biolreprod.110.086181

BIOLOGY OF REPRODUCTION **84,** 801–815 (2011)
Published online before print 22 September 2010.
DOI 10.1095/biolreprod.110.086181

Unique Transcriptome, Pathways, and Networks in the Human Endometrial Fibroblast Response to Progesterone in Endometriosis[1]

L. Aghajanova,[3,4] K. Tatsumi,[3,4] J.A. Horcajadas,[4] A.M. Zamah,[4] F.J. Esteban,[5] C.N. Herndon,[4] M. Conti,[4] and L.C. Giudice[2,4]

Department of Obstetrics, Gynecology and Reproductive Sciences,[4] University of California San Francisco, San Francisco, California
Department of Experimental Biology,[5] University of Jaen, Jaen, Spain

ABSTRACT

Eutopic endometrium in endometriosis has molecular evidence of resistance to progesterone (P_4) and activation of the PKA pathway in the stromal compartment. To investigate global and temporal responses of eutopic endometrium to P_4, we compared early (6-h), intermediate (48-h), and late (14-Day) transcriptomes, signaling pathways, and networks of human endometrial stromal fibroblasts (hESF) from women with endometriosis ($hESF_{endo}$) with hESF from women without endometriosis ($hESF_{nonendo}$). Endometrial biopsy samples were obtained from subjects with and without mild peritoneal endometriosis (n = 4 per group), and hESF were isolated and treated with P_4 (1 μM) plus estradiol (E_2) (10 nM), E_2 alone (10 nM), or vehicle for up to 14 days. Total RNA was subjected to microarray analysis using a Gene 1.0 ST (Affymetrix) platform and analyzed by using bioinformatic algorithms, and data were validated by quantitative real-time PCR and ELISA. Results revealed unique kinetic expression of specific genes and unique pathways, distinct biological and molecular processes, and signaling pathways and networks during the early, intermediate, and late responses to P_4 in both $hESF_{nonendo}$ and $hESF_{endo}$, although a blunted response to P_4 was observed in the latter. The normal response of hESF to P_4 involves a tightly regulated kinetic cascade involving key components in the P_4 receptor and MAPK signaling pathways that results in inhibition of E_2-mediated proliferation and eventual differentiation to the decidual phenotype, but this was not established in the $hESF_{endo}$ early response to P_4. The abnormal response of this cell type to P_4 may contribute to compromised embryonic implantation and infertility in women with endometriosis.

decidualization, endometrial fibroblast, endometriosis, eutopic endometrium, progesterone, transcriptome

INTRODUCTION

Endometriosis, a common gynecologic disorder, is characterized by endometrium-like tissue on the pelvic peritoneum, ovary, and rectovaginal septum. It is present in up to 60% of women with chronic pelvic pain and dysmenorrhea and up to 50% of women with infertility [1, 2]. Retrograde transplantation of steroid hormone-sensitive endometrial tissue and cells into the pelvic cavity at the time of menses is believed to account for peritoneal disease and is accompanied by a local inflammatory response that contributes to the observed pain and infertility [3]. This shed eutopic endometrium of women with endometriosis has different innate properties that likely contribute to its attachment to, invasion of, and growth on peritoneal structures, giving rise to the disorder in genetically, environmentally, and immunologically predisposed individuals [4, 5]. Eutopic endometrium is composed of several cell types that respond to the circulating steroid hormones estradiol (E_2) and progesterone (P_4) in preparation for blastocyst nidation, placentation, and sustainability of an established pregnancy. The human endometrial stromal fibroblast (hESF), in response to P_4 after E_2 priming, undergoes distinct morphological differentiation, with changes in the cytoskeleton and a functional transition from fibroblast-like to epithelium-like cells, which is accompanied by a unique biosynthetic and secretory phenotype, and plays a critical role in successful embryonic implantation [6]. When pregnancy ensues, the endometrial stromal compartment becomes uniformly ''decidualized'' and constitutes the decidua, a morphologically and functionally distinct tissue that persists throughout gestation and represents the maternal aspect of the maternal-fetal interface, composed of decidualized stromal fibroblasts, vascular elements, epithelium, and immune cells [7]. Through their responses to P_4, hESF communicate with the extracellular matrix, the invading trophoblast, and resident and peripheral leukocyte populations in the developing placental bed [8]. Thus, an abnormal hESF differentiation program can affect the success of implantation, early development, and pregnancy. In the setting of endometriosis, this differentiation program is compromised [4, 9].

hESF responses to P_4 are complex and involve activation of PKA, the progesterone receptor (*PGR*) gene, and other pathways, with cross-talk between and among them [9–11], a consequence of P_4 binding to its cognate nuclear receptors, and nongenomic mechanisms [12, 13]. Resistance to P_4 actions in eutopic endometrium of women with endometriosis is believed to derive from lower levels of *PGRA, PGRB* [14, 15], and *PGR* coregulator expression [10], aberrant expression of specific transcription factors [16–18], and dysregulation of members and functions of specific pathways that drive hESF toward decidualization [4, 9, 19, 20]. We and others have demonstrated that hESF from women with endometriosis exhibit a blunted

[1]Supported by Eunice Kennedy Shriver National Institute of Child Health and Human Development/National Institutes of Health cooperative agreement 1U54HD055764-04, as part of the Specialized Cooperative Centers Program in Reproduction and Infertility Research, to L.C.G.
[2]Correspondence: FAX: 415 476 6203;
e-mail: giudice@obgyn.ucsf.edu
[3]These authors contributed equally to this work.

Received: 22 May 2010.
First decision: 21 June 2010.
Accepted: 2 September 2010.

eISSN: 1529-7268 http://www.biolreprod.org
ISSN: 0006-3363

TABLE 1. Subject characteristics for this study.

Patient	hESF used in experiments[a]	Diagnosis at laparoscopy	Age (yr)	Ethnicity
233[b]	Microarray, ELISA, validation	Mild endometriosis, pelvic pain	31	Caucasian
243[b]	Microarray, ELISA, validation	Minimal endometriosis, bilateral ovarian cyst, intramural myoma	46	Caucasian
267[b]	Microarray, ELISA, validation	Mild endometriosis, pelvic pain	32	Caucasian
270	Microarray, ELISA, validation	Mild endometriosis, pelvic pain	49	Caucasian
236[b]	Microarray, ELISA, validation	Symptomatic pelvic prolapse	47	Caucasian
310	Microarray, ELISA, validation	Intramural myoma, enterocele	41	Asian
316	Microarray, ELISA, validation	Intramural myoma, adenomyosis	42	Caucasian
326[b]	Microarray, ELISA, validation	Intramural myoma	49	Asian

[a] ELISA, enzyme-linked immunoassay.
[b] hESF as used in the study by Giudice [8].

response to activation of the PKA pathway [9, 19]. However, it is unclear what the global response to P_4 per se is in the impaired decidualization observed in hESF from women with endometriosis.

Thus, a comparative investigation of genes, gene families, and signaling and biological pathways involved in the hESF response to P_4 in women with and without endometriosis is important to understand the mechanisms underlying normal and abnormal implantation and pregnancy maintenance. Herein, we compared early (6-h), intermediate (48-h), and late (14-Day) in vitro whole-genome responses of hESF from women with endometriosis ($hESF_{endo}$) to hESF from women without endometriosis ($hESF_{nonendo}$) treated with P_4 plus E_2 (E_2P_4), or E_2 alone, or vehicle alone. Using this experimental paradigm, the data demonstrate unique phenotypes, gene expression processes, biochemical and signaling pathways, and networks suggestive of early, intermediate, and late responses of $hESF_{nonendo}$ and $hESF_{endo}$ to P_4, giving insights into the complexity of events occurring normally in response to P_4 and in the setting of endometriosis.

MATERIALS AND METHODS

Tissues and Cells

Endometrial tissue samples were obtained in accordance with the guidelines of the Declaration of Helsinki. Written, informed consent was obtained from all subjects. The study was approved by the Committee on Human Research of the University of California San Francisco (UCSF) and the Stanford University Committee on the Use of Human Subjects in Medical Research. Some samples were also obtained from the National Institutes of Health Specialized Cooperative Centers Program in Reproduction and Infertility Research (SCCPRR) Human Endometrial Tissue and DNA Bank at UCSF. Control subjects were premenopausal women (44.75 ± 1.7 years old; range 41–49 years old) undergoing hysterectomy for benign conditions (Table 1), with regular menstrual cycles (25–35 days), surgically confirmed absence of endometriosis, and no history of endometriosis. Endometriosis subjects were 39.5 ± 4.2-year-old (range, 31–49 years old; $P = 0.35$, vs. $hESF_{nonendo}$ subjects) women with regular menstrual cycles, in whom minimal to mild peritoneal endometriosis was diagnosed by visualization of pelvic lesions during laparoscopy and histologic evaluation (Table 1). Endometriosis was staged according to the revised American Fertility Society classification system [21]. All subjects were documented not to be pregnant and not to have had hormonal treatment for at least 3 months before surgery.

Endometrial tissue was digested with collagenase, and hESF were isolated and plated with Dulbecco modified Eagle medium (DMEM)/molecular cell developmental biology 105 (MCDB-105) medium with 10% charcoal-stripped fetal bovine serum (FBS), insulin (5 mg/ml), gentamicin, penicillin, and streptomycin, as described previously [22, 23]. All cells used were at Passage 2. Subsequently, hESF were plated in 6-cm plastic dishes, and, after they reached confluency, medium was changed to a low-serum medium (LSM; i.e., DMEM/MCDB-105 medium containing ascorbic acid, transferrin, and gentamicin with 2% FBS) for 24 h prior to treatment. The concentration of FBS (2%) in the culture medium was determined by culturing two preparations in triplicate for up to 16 days with 1μM P_4 plus 10 nM E_2 (E_2P_4) in 0%, 0.5%, 1%, 2%, 5%, and 10% FBS, and the classical decidual marker IGFBP1, in conditioned medium (CM) was measured by ELISA (Diagnostic Systems Labs, Webster, TX). Optimal IGFBP1 secretion was observed in the culture with 2% FBS (data not shown).

Hormonal Treatment, RNA Isolation, and Processing for Microarray Analysis

Figure 1 shows the experimental design of the present study. Duplicate cultures of hESF in LSM were treated with E_2P_4 or with 10 nM E_2 alone (E_2) or with vehicle (vehicle control), and cells and CM were collected at time (*t*) of 0 h, 6 h (early response), 48 h (intermediate response), and 14 days (late response), and CM was changed every 2 days. Total RNA was isolated from

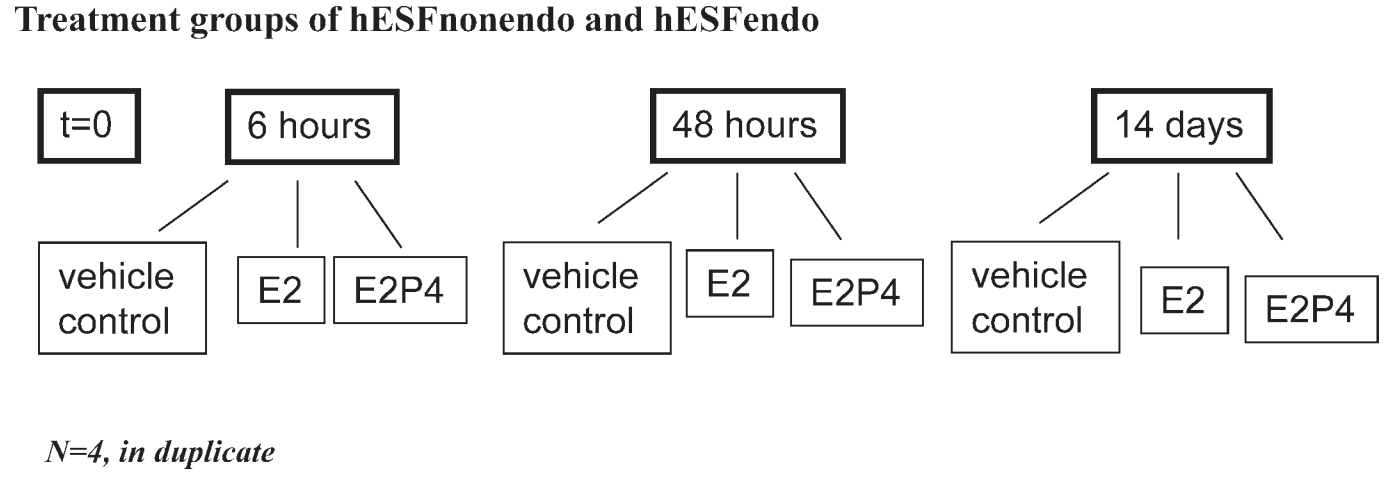

FIG. 1. Experimental design. Treatment groups were similar for $hESF_{nonendo}$ and $hESF_{endo}$. For analysis of microarray and QRT-PCR data, all groups were normalized to $t = 0$, and then the normalization was conducted within each time-group: E_2P_4 was normalized to E_2, which was normalized to the vehicle control, with the resulting data reflecting the pure P_4 response.

TABLE 2. Primer sequences used in real-time RT-PCR experiments.

Gene	Sense primer 5′–3′	Antisense primer 5′–3′
IGFBP1	CTATGATGGCTCGAAGGCTC	TTCTTGTTGCAGTTTGGCAG
PRL	CATCAACAGCTGCCACACTT	CGTTTGGTTTGCTCCTCAAT
GPX3	AGCCGGGGACAAGAGAAGT	CCAGAATGACCAGACCGAAT
SLC7A8	ACCGAAACAACACCGAAAAG	GATTCCAGAGCCGATGATGT
IMPA2	TGGGAGGAGTGCTTCCAG	GCCTCTTCTGCAATGAACCT
CNR1	AAGACCCTGGTCCTGATCCT	CGCAGGTCCTTACTCCTCAG
SPARCL1	GGATGAAAAGAGGCTTTTGG	TCAAAGAAACGGGTTATGCAG
EGFR	GAATGCATTTGCCAAGTCCT	CGTCTATGCTGTCCTCAGTCA
DKK1	CATCAGACTGTGCCTCAGGA	CCACAGTAACAACGCTGGAA
ERRFI1 (MIG6)	TTGCTGCTCAGGAGATCAGA	TTCAGACTGTAGGCCATGGTT
RPL19	GCAGATAATGGGAGGAGCC	GCCCATCTTTGATGAGCTTC

individual plates and purified using an RNeasy mini-kit (Qiagen, Valencia, CA) following the manufacturer's protocol. Samples were stored in RNase-free H_2O, purity was analyzed by the A_{260}:A_{280} nm ratio, and RNA quality and integrity were assessed by using a Bioanalyzer 2100 unit (Agilent Technologies, Santa Clara, CA). All samples had high-quality RNA (RNA integrity number [RIN] = 9.7–10).

Duplicate RNA preparations were pooled and prepared according to the manufacturer's microarray preparation protocol (Affymetrix, Inc., Santa Clara, CA) as described previously [9]. Briefly, for each sample, 100 ng of total RNA was reverse-transcribed to cDNA by using 500 ng of T7-(N6) primer and SuperScript II. A second strand of DNA was generated using DNA polymerase, followed by overnight in vitro transcription to generate cRNA. After samples were processed through cRNA clean-up spin columns (Affymetrix), 10 μg of cRNA was reverse-transcribed using random primers and SuperScript II. Mixtures were digested with RNase H, and cDNA was purified by cDNA clean-up spin columns (Affymetrix). Finally, 5.5 μg of sense cDNA was fragmented and labeled using a GeneChip WT-terminal labeling kit. The quality of the cDNA and the fragmented cDNA was assessed with an Agilent bioanalyzer. Individual samples were hybridized to Human Gene 1.0 ST arrays (Affymetrix) containing 19 492 genes. Data were scanned according to the protocol described in the WT sense target-labeling assay manual from Affymetrix (version 4; product code FS450_0007).

Microarray Gene Expression Data Analysis

The intensity values of different probe sets (genes) in the GeneChip operating software (Affymetrix) were imported into GeneSpring GX version 10.0 software (Agilent Technologies, Santa Clara, CA) and processed using the robust multiarray analysis algorithm for background adjustment, normalization, and log2 transformation of perfect-match values [9, 24]. The data at each time point were normalized to the corresponding sample at $t = 0$ h. Then, the normalization was conducted within each time-group: data from E_2P_4-treated samples were normalized to those from E_2-treated samples, which were normalized to the vehicle control, with the resulting data thus reflecting the specific temporal response to P_4. We performed three major comparisons of the response to P_4: within the nonendometriosis group, within the endometriosis group, and between $hESF_{endo}$ and $hESF_{nonendo}$. The resulting gene lists generated included only genes showing >1.5-fold change in expression and a P value of <0.05 by using a two-way ANOVA parametric test and Benjamini-Hochberg multiple testing correction for false discovery rate.

Principal Component Analysis and Hierarchical Clustering

Principal component analysis (PCA) and hierarchical clustering were performed as described previously [9, 24]. We applied the unbiased PCA algorithm in GeneSpring software to all samples, using all 19 492 genes on the Human Gene 1.0 ST array chip to look for similar expression patterns and underlying cluster structures. Hierarchical cluster analysis uses only differentially expressed genes from all samples and from among all experimental conditions and was conducted using the smooth-correlation-distance-measure algorithm (GeneSpring) to identify samples with similar patterns of gene expression.

Gene Ontology and Pathway Analyses

Gene ontology and functional annotations were carried out using Ingenuity Pathway analysis (IPA) (Ingenuity Systems, Redwood City, CA), into which gene symbols and fold changes of up- and downregulated genes in each pair-wise comparison were imported [9].

Microarray Validation by Real-Time PCR

Genes showing >1.5-fold up- or downregulation at each time point were randomly chosen for validation by quantitative real-time PCR (QRT-PCR). QRT-PCR assays were performed in duplicate using SYBR Green PCR Master Mix (Bio-Rad Laboratories, Hercules, CA) according to the manufacturer's instructions. The *RPL19* housekeeping gene was used as the normalizer. Primer sequences (Table 2) were designed from public databases, and PCR assays were run using Mx4000 and Mx3005 QPCR systems (Stratagene, La Jolla, CA) under thermal cycling conditions as described previously [9, 22]. Pair-wise comparisons between treatments and control at each time point were performed. All validation experiments used four-subject samples in each group. Statistical analysis for the QRT-PCR assays was performed using the nonparametric Mann-Whitney U-test. Significance was determined at a P value of ≤ 0.05.

ELISA

ELISAs were carried out to quantify IGFBP1 (Alpha Diagnostic International, San Antonio, TX), PRL (Diagnostic Systems Labs, Webster, TX), and amphiregulin (AREG) and HBEGF (both, R&D Systems Inc., Minneapolis, MN) levels in CM from cultured hESF, performed according to manufacturers' instructions. All samples were assayed in duplicate, and values were plotted against a standard curve. Levels of IGFBP1, PRL, AREG, and HBEGF expression in CM for each sample were normalized to total RNA. The IGFBP1 ELISA kit had inter- and intra-assay coefficient of variation values (CV) of 5%–7.4% and 2.4%–3.4%, respectively, and the PRL ELISA inter- and intra-assay CVs were 6.7%–10.4% and 7.8%–8.2%, respectively. The sensitivity for the AREG ELISA was 15 pg/ml, with a linear range up to 1000 pg/ml. The sensitivity for the HBEGF ELISA was 30 pg/ml, with a linear range up to 2000 pg/ml. Statistical analysis of the ELISA data was performed using a two-tailed type 3 Student-t test.

RESULTS

PCA and Hierarchical Clustering Analysis

PCA distributes samples into a three-dimensional space based on variations in gene expression, with samples that have similar gene expression profile trends clustering close together. When we used all genes on the Affymetrix array and a completely unbiased approach, the samples roughly clustered into two major groups, in a comparison of disease versus no disease (Fig. 2A).

Unsupervised hierarchical clustering analyses based on the combined gene list derived from pair-wise comparisons as described above (Fig. 1) at each time point resulted in a dendrogram of sample clustering and a heat map of gene expression (Fig. 2B) in which all control samples ($t = 0$ h and vehicle control) and all treated samples fell into two main branches. Short-term treatment (6-h) groups (vehicle control, E_2-treated, and E_2P_4-treated) clustered together in one sub-branch with $t = 0$. Intermediate (48-h) and long-term (14-Day) treatment groups clustered into other main sub-branches; the latter group clustered further into two sub-branches, based on the disease state, followed by further

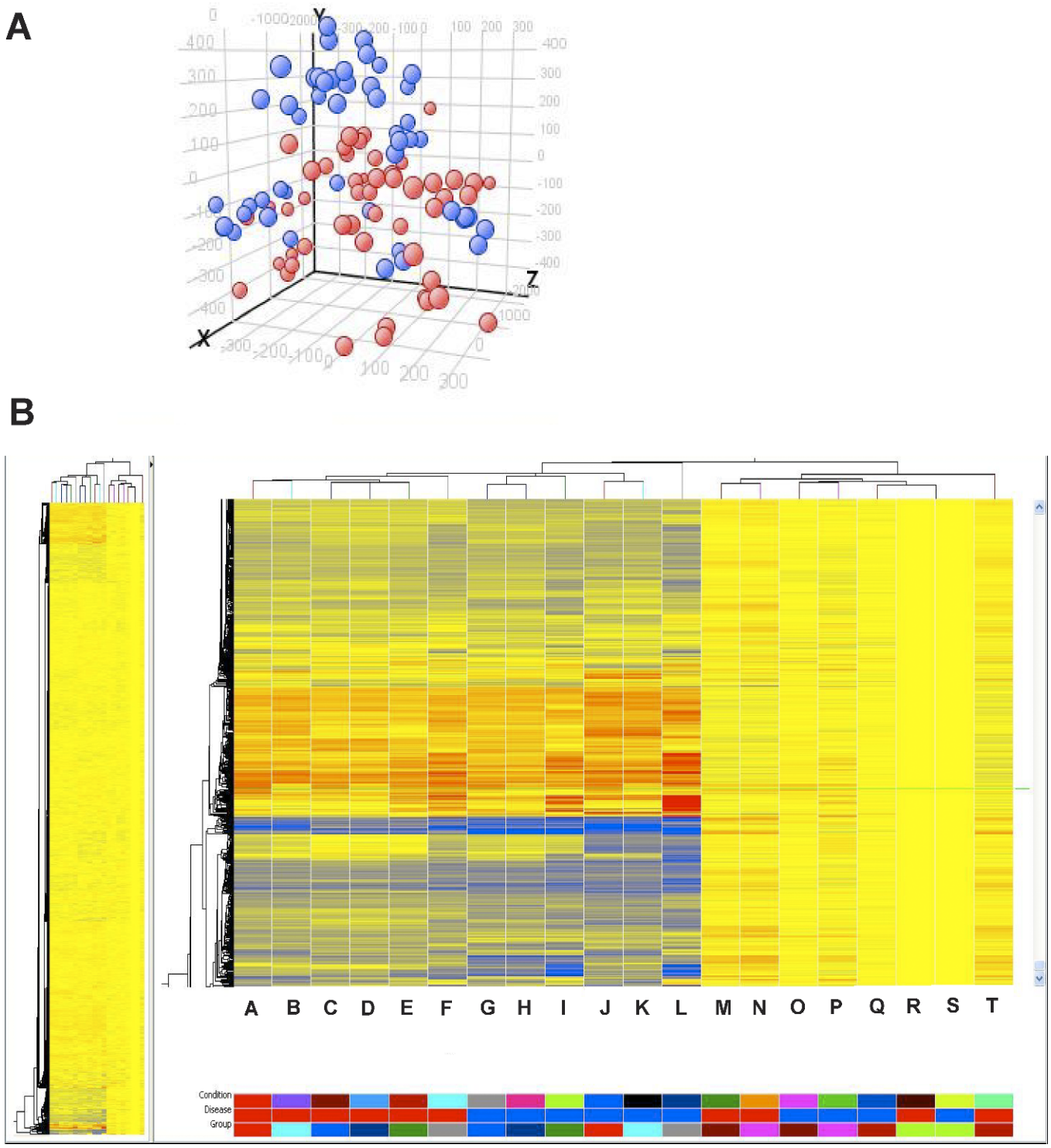

FIG. 2. Clustering and cluster trees. **A**) Principal component analysis of $hESF_{nonendo}$ and $hESF_{endo}$ at $t = 0$, 6, and 48 h and at 14 days, treated with or without E_2 and P_4. PCA was applied to all samples that were characterized by the gene expression of all probes on a Gene 1.0 ST platform. Blue, no endometriosis samples; red, endometriosis samples. **B**) Hierarchical clustering analysis of $hESF_{nonendo}$ and $hESF_{endo}$ at $t = 0$, 6, and 48 h and at 14 days, treated with or without (control [c]) estrogen (E_2), and progesterone (P_4), using only the profiles of significantly regulated genes. The heat map represents relative expression levels of genes in the hESF samples: each horizontal line represents a single gene, and each column represents a single sample. The relative expression of each gene is color coded as high (red) or low (blue) or no change (yellow). Groups: A, E_2 14-Day endo; B, c 14-Day endo; C, E_2 48-h endo; D, c 48-h endo; E, E_2P_4 48-h endo; F, E_2P_4 14-Day endo; G, E_2 48-h nonendo; H, c 48-h nonendo; I, E_2P_4 48-h nonendo; J, E_2 14-Day nonendo; K, c 14-Day nonendo; L, E_2P_4 14-h nonendo; M, E_2 6-h endo; N, E_2P_4 6-h endo; O, E_2 6-h nonendo; P, E_2P_4 6-h nonendo; Q, c 6-h nonendo; R, $t = 0$ endo; S, $t = 0$ nonendo; T, c 6-h endo.

TABLE 3. List of up- and downregulated genes (BH corrected P value < 0.05) in comparison of $hESF_{endo}$ at $t = 0$ ($hESF_{endo}$ $t = 0$) versus $hESF_{nonendo}$ at $t = 0$, expressed as fold change (FC).

Gene symbol	FC ([endometriosis-t0] vs. [nonendometriosis-t0])	Gene description
CNIH3	2.35	Cornichon homolog 3 (Drosophila)
ANKRD1	2.14	Ankyrin repeat domain 1 (cardiac muscle)
AREG	2.12	Amphiregulin (schwannoma-derived growth factor)
TGFB2	1.81	Transforming growth factor, beta 2
CLDN1	1.79	Claudin 1
HBEGF	1.71	Heparin-binding EGF-like growth factor
ITGA2	1.67	Integrin, alpha 2 (CD49B, alpha 2 subunit of VLA-2 receptor)
NEDD4L	1.61	Neural precursor cell expressed, developmentally down-regulated 4-like
HS3ST3B1	1.58	Heparan sulfate (glucosamine) 3-O-sulfotransferase 3B1
SLC20A1	1.58	Solute carrier family 20 (phosphate transporter), member 1
ANKH	1.57	Ankylosis, progressive homolog (mouse)
STC2	1.57	Stanniocalcin 2
RGS4	1.56	Regulator of G-protein signaling 4
TM7SF4	1.55	Transmembrane 7 superfamily member 4
UNQ1940	1.55	HWKM1940
SLC16A6	1.50	Solute carrier family 16, member 6 (monocarboxylic acid transporter 7)
FKBP5|LOC285847	−1.50	FK506 binding protein 5 | hypothetical protein LOC285847
C10orf10	−1.50	Chromosome 10 open reading frame 10
CCNE2	−1.50	Cyclin E2
SEPP1	−1.50	Selenoprotein P, plasma, 1
SULF2	−1.51	Sulfatase 2
C4orf31	−1.52	Chromosome 4 open reading frame 31
IL1R1	−1.54	Interleukin 1 receptor, type I
OSR2	−1.54	Odd-skipped related 2 (Drosophila)
ARHGAP28	−1.54	Rho GTPase activating protein 28
TMEM16D	−1.55	Transmembrane protein 16D
RASL11A	−1.55	RAS-like, family 11, member A
CYB5A	−1.55	Cytochrome b5 type A (microsomal)
MYLIP	−1.56	Myosin regulatory light chain interacting protein
FMO2	−1.57	Flavin containing monooxygenase 2 (non-functional)
LRRK2	−1.57	Leucine-rich repeat kinase 2
ACTA2	−1.58	Actin, alpha 2, smooth muscle, aorta
KGFLP1|KGFLP2|LOC100126582|FGF7P2|FLJ20444|LOC100132771|LOC100133691	−1.58	Keratinocyte growth factor-like protein 1 | keratinocyte growth factor-like protein 2
METTL7A	−1.59	Methyltransferase like 7A
KGFLP2|KGFLP1|FGF7P2|FLJ20444|LOC100132771|LOC100133691	−1.60	Keratinocyte growth factor-like protein 2 | keratinocyte growth factor-like protein 1
UST	−1.61	Uronyl-2-sulfotransferase
CD226	−1.62	CD226 molecule
LMOD1	−1.62	Leiomodin 1 (smooth muscle)
RORB	−1.64	RAR-related orphan receptor B
ABI3BP	−1.64	ABI gene family, member 3 (NESH) binding protein
PRLR	−1.67	Prolactin receptor
ABCC9	−1.67	ATP-binding cassette, sub-family C (CFTR/MRP), member 9
IFIT1	−1.68	Interferon-induced protein with tetratricopeptide repeats 1
TACSTD2	−1.68	Tumor-associated calcium signal transducer 2
ITGB8	−1.75	Integrin, beta 8
PGR	−1.76	Progesterone receptor
ENPP1	−1.76	Ectonucleotide pyrophosphatase/phosphodiesterase 1
RASGRP1	−1.87	RAS guanyl releasing protein 1 (calcium and DAG-regulated)
TNC	−1.89	Tenascin C (hexabrachion)
SMPDL3A	−1.90	Sphingomyelin phosphodiesterase, acid-like 3A
SLC40A1	−1.94	Solute carrier family 40 (iron-regulated transporter), member 1
C1R	−1.99	Complement component 1, r subcomponent
CPM	−2.04	Carboxypeptidase M
IL7R	−2.11	Interleukin 7 receptor
PLXNC1	−2.11	Plexin C1
NEFM	−2.21	Neurofilament, medium polypeptide 150kDa
FBLN1	−2.30	Fibulin 1

branching according to the treatment time (Fig. 2B). This clustering demonstrates that cultured, treated hESF cluster according to the duration of hormonal exposure, similar to in vivo hormonal exposure of whole-tissue samples, which cluster based primarily on cycle phase [24, 25] and thereafter based on disease state [25].

Differences in Gene Expression Between $hESF_{endo}$ and $hESF_{nonendo}$ at $t = 0$

Comparisons between gene expression in $hESF_{endo}$ and $hESF_{nonendo}$ at $t = 0$ (untreated uncultured control) revealed differences between the two (Table 3). In particular, we observed upregulation of members of the *EGF* and *TGFB*

families (*HBEGF*, *AREG*, *TGFB2*), the *SLC16A6* solute carrier, and the neural precursor cell expressed developmentally downregulated 4-like (*NEDD4L*) gene in $hESF_{endo}$ compared with the $hESF_{nonendo}$ samples. Also, there was significant downregulation of several genes at $t = 0$ in $hESF_{endo}$ versus $hESF_{nonendo}$, including the *FKBP5*, *IL1R1*, sulfatase 2, prolactin receptor, methyltransferase-like 7A, and plexin C1 genes; the cytoskeletal *MYLIP* and *ACTA2* genes; and the progesterone receptor (*PGR* [1.75-fold]) gene (Table 3). IPA analysis of the comparison of these groups showed that the *HBEGF* and *AREG* genes were allocated to several different signaling pathways, including neuregulin signaling, ERBB2 (HER-2) signaling in breast cancer, pancreatic adenocarcinoma signaling, and others. Analysis of hESF transcriptomes at $t = 0$ revealed no gene profile was unique to one menstrual cycle phase versus another (data not shown), consistent with previous reports [22].

Early, Intermediate, and Late Responses to P_4

We investigated the temporal responses presumably to P_4 (by comparison of E_2P_4 vs. E_2 response) of $hESF_{nonendo}$ and $hESF_{endo}$ and then compared the two responses to each other. These comparisons enabled us to define the ''normal'' P_4-regulated program from early response genes to the full decidual phenotype, as well as the $hESF_{endo}$ response.

Early Response

$hESF_{nonendo}$. In a comparison of $hESF_{nonendo}$ treated with E_2P_4 versus E_2 alone, upregulated genes included the *SLC7A8* solute carrier, the *PGR FKBP5* chaperone, the *SPARCL1* gene, the ERBB receptor feedback inhibitor 1 (*ERRFI1*, *MIG6*), *IMPA2*, and *GCNT1* genes, the adrenergic alpha-2C receptor, and chromosome 10 open reading frame 10 (*C10orf10*), among others (Table 4). There were no significantly downregulated genes at the 1.5-fold change cutoff.

$hESF_{endo}$. Analysis of microarray data of gene expression after 6 h of treatment in $hESF_{endo}$ revealed no genes were up- or downregulated at the >1.5-fold cutoff ($P < 0.05$) (Table 4). Interestingly, in the E_2-treated groups, the E_2 target *PGR* gene was upregulated in $hESF_{nonendo}$ at 6 h, demonstrating early responsiveness to E_2; however, in $hESF_{endo}$, there was delayed *PGR* upregulation, first noted at 48 h of E_2 treatment (data not shown). This time shift in E_2 regulation of the *PGR* gene may account for the relative resistance to P_4 observed in $hESF_{endo}$ at the 6-h time point of cells treated with E_2P_4. Importantly, the early response to P_4 (E_2P_4 vs. E_2) signaling involving the *PGR* chaperone and the MAPK pathway was not established in $hESF_{endo}$.

Intermediate Response

$hESF_{nonendo}$. In a comparison of E_2P_4- and E_2-treated $hESF_{nonendo}$ at 48 h, in addition to the sustained or enhanced upregulation of the early response genes already described above at 6 h, the first upregulation was observed for the *IGF1*, *DKK1*, *KLF6*, *MAOB*, *IL1R1*, ectonucleotide pyrophosphatase/phosphodiesterase 1 (*ENPP1*) (regulator of extracellular inorganic pyrophosphate [PPi]), sulfatase 2, plexin C1, and osteomodulin genes and others (Table 4). Among the downregulated were the *SLC16A6* soluble carrier, the *MMP11*, and the dual-specificity phosphatase 6 genes and others (Table 4).

$hESF_{endo}$. In $hESF_{endo}$, there were only three significantly upregulated genes: the *IMPA2* (upregulated in $hESF_{nonendo}$ at 6 h), methyltransferase-like 7A, and *IL1R1* genes (Table 4).

Late Response

$hESF_{nonendo}$. After $hESF_{nonendo}$ was treated for 14 days, in addition to the continued or enhanced expression of the genes mentioned above, the uniquely upregulated (>1.5-fold, $P < 0.05$) group included the classical P_4-regulated *PRL*, *IGFBP1*, *GPX3*, *MAOA*, tenascin family, prolactin receptor, parathyroid hormone-like hormone, adenylate cyclase 1, hydroxysteroid (17-beta) dehydrogenase type 11 (*HSD17B11*), and *FOXO1A* genes and others (Table 5). Among those newly observed and significantly downregulated were the *IGFBP5*, cyclin D1, neurofilament medium polypeptide (*NEFM*), and pleiotrophin (*PTN*, heparin-binding growth factor 8, neurite growth-promoting factor 1) genes and others (Table 5).

$hESF_{endo}$. In contrast, in $hESF_{endo}$, only a few P_4-dependent genes were (up)regulated, including the *C10orf10*, *SLC7A8* (both upregulated at 6 h in $hESF_{nonendo}$), *ADH1B* (upregulated at 48 h in $hESF_{nonendo}$), and *IL1R1* genes (Table 5).

Validation of Microarray Data by RT-PCR

To validate microarray data by QRT-PCR, we randomly selected nine genes from the microarray data analysis: *IGFBP1*, *PRL*, *IMPA2*, *SLC7A8*, *DKK1*, *GPX3*, *ERRFI1 (MIG6)*, *SPARCL1*, and *CNR1* (Fig. 3). There was very high concordance of gene regulation observed in the microarray analysis and the validation studies. We confirmed significant dysregulation of P_4-regulated endometrial genes, such as *IGFBP1*, *IMPA2*, *SLC7A8*, *GPX3*, *ERRFI1*, *SPARCL1*, and *CNR1*, in $hESF_{endo}$ compared to those in $hESF_{nonendo}$ in response to E_2P_4 versus E_2 treatment, even at earlier time points (Fig. 3).

Validation of Microarray Data by ELISA

IGFBP1 and PRL. Secretion of the IGFBP1 decidualization marker, but not PRL, in response to E_2P_4 versus E_2 treatment differed between $hESF_{endo}$ and $hESF_{nonendo}$ (Fig. 4), confirming the mRNA validation data (Fig. 3).

Amphiregulin and heparin-binding EGF-like growth factor secretion by hESF. Previous publications have implicated the EGF signaling network in the pathogenesis of endometriosis [25, 26]. Because amphiregulin (*AREG*) and heparin-binding EGF-like growth factor (*HBEGF*) transcripts were upregulated in $hESF_{endo}$ versus $hESF_{nonendo}$ at $t = 0$ and at 6 h (Table 3, Supplemental Table S1 [available online at www.biolreprod.org]), we measured AREG and HBEGF protein in CM of hESF. No detectable AREG protein was found in CM from $hESF_{nonendo}$ at any time point or from any treatment group. However, all $hESF_{endo}$ secreted AREG (data not shown). There was a tendency toward increased AREG expression with time; however, differences from one time point to another were not significant, and there was no apparent effect of hormonal treatment on AREG levels in CM (data not shown), suggesting constitutive expression of this growth factor in $hESF_{endo}$. There was no HBEGF protein detected in CM from hormonally treated and control $hESF_{nonendo}$ at different time points, and $hESF_{endo}$ secretion levels of HBEGF in CM were at the lower limit of detection of the assay (data not shown).

Early and Late Responses in $hESF_{endo}$ Versus $hESF_{nonendo}$: Canonical Pathways and Networks

The degree of regulation of signaling pathways and network formations in different comparison groups depends on the total number of genes regulated in each group (see gene lists in

TABLE 4. List of regulated genes (BH corrected P value < 0.05) in comparison of $hESF_{nonendo}$ or $hESF_{endo}$ treated with E_2P_4 for 6-h (EP6) or 48-h (EP48) versus $hESF_{nonendo}$ or $hESF_{endo}$ treated with E_2 for 6-h (E6) or 48-h (E48), expressed as fold change (FC).[a]

Gene symbol	FC	Gene description
$hESF_{nonendo}$ EP6 vs. $hESF_{nonendo}$ E6		
FKBP5|LOC285847	1.99	FK506 binding protein 5 | hypothetical protein LOC285847
IMPA2	1.67	Inositol(myo)-1(or 4)-monophosphatase 2
SLC7A8	1.67	Solute carrier family 7 (cationic amino acid transporter, y+ system), member 8
ERRFI1	1.61	ERBB receptor feedback inhibitor 1
GCNT1	1.56	Glucosaminyl (N-acetyl) transferase 1, core 2 (beta-1,6-N-acetylglucosaminyltransferase)
SPARCL1	1.56	SPARC-like 1 (mast9, hevin)
C10orf10	1.54	Chromosome 10 open reading frame 10
ADRA2C	1.51	Adrenergic, alpha-2C-, receptor
$hESF_{nonendo}$ EP48 vs. $hESF_{nonendo}$ E48		
P2RY14	3.37	Purinergic receptor P2Y, G-protein coupled, 14
IGF1	3.11	Insulin-like growth factor 1 (somatomedin C)
ENPP1	2.98	Ectonucleotide pyrophosphatase/phosphodiesterase 1
FKBP5|LOC285847	2.98	FK506 binding protein 5 | hypothetical protein LOC285847
MYOCD	2.97	Myocardin
IMPA2	2.95	Inositol(myo)-1(or 4)-monophosphatase 2
ADH1B	2.86	Alcohol dehydrogenase 1B (class I), beta polypeptide
RORB	2.67	RAR-related orphan receptor B
ADRA2C	2.21	Adrenergic, alpha-2C-, receptor
ABI3BP	2.18	ABI gene family, member 3 (NESH) binding protein
MOBKL2B	2.15	MOB1, Mps One Binder kinase activator-like 2B (yeast)
SPARCL1	2.14	SPARC-like 1 (mast9, hevin)
SLC7A8	2.05	Solute carrier family 7 (cationic amino acid transporter, y+ system), member 8
IL1R1	2.02	Interleukin 1 receptor, type I
METTL7A	2.00	Methyltransferase like 7A
ACSL1	1.95	Acyl-CoA synthetase long-chain family member 1
LASS6	1.93	LAG1 homolog, ceramide synthase 6
CRISPLD2	1.91	Cysteine-rich secretory protein LCCL domain containing 2
ERRFI1	1.91	ERBB receptor feedback inhibitor 1
ADAMTS1	1.88	ADAM metallopeptidase with thrombospondin type 1 motif, 1
SERPINE1	1.88	Serpin peptidase inhibitor, clade E (nexin, plasminogen activator inhibitor type 1), member 1
APCDD1	1.87	Adenomatosis polyposis coli down-regulated 1
C10orf10	1.86	Chromosome 10 open reading frame 10
MUM1L1	1.84	Melanoma associated antigen (mutated) 1-like 1
ZBTB16	1.83	Zinc finger and BTB domain containing 16
NBLA00301	1.80	Nbla00301
NLGN4X	1.77	Neuroligin 4, X-linked
ABCC9	1.76	ATP-binding cassette, sub-family C (CFTR/MRP), member 9
TSC22D3	1.74	TSC22 domain family, member 3
CCDC102B	1.73	Coiled-coil domain containing 102B
ADH1C	1.73	Alcohol dehydrogenase 1C (class I), gamma polypeptide
SORBS1	1.71	Sorbin and SH3 domain containing 1
PPAP2B	1.64	Phosphatidic acid phosphatase type 2B
OMD	1.63	Osteomodulin
OSR2	1.61	Odd-skipped related 2 (Drosophila)
TLR4	1.60	Toll-like receptor 4
PLXNC1	1.58	Plexin C1
HAND2	1.56	Heart and neural crest derivatives expressed 2
DKK1	1.56	Dickkopf homolog 1 (*Xenopus laevis*)
MAOB	1.55	Monoamine oxidase B
C5orf23	1.55	Chromosome 5 open reading frame 23
NPR3	1.54	Natriuretic peptide receptor C/guanylate cyclase C (atrionatriuretic peptide receptor C)
KLF6	1.53	Kruppel-like factor 6
SYTL4	1.53	Synaptotagmin-like 4 (granuphilin-a)
SULF2	1.52	Sulfatase 2
RHOU	1.52	Ras homolog gene family, member U
ZEB1	1.50	Zinc finger E-box binding homeobox 1
SLC16A6	−1.50	Solute carrier family 16, member 6 (monocarboxylic acid transporter 7)
AFAP1L2	−1.53	Actin filament associated protein 1-like 2
MMP11	−1.59	Matrix metallopeptidase 11 (stromelysin 3)
CCRL1	−1.60	Chemokine (C-C motif) receptor-like 1
FJX1	−1.61	Four jointed box 1 (Drosophila)
KRT34	−1.61	Keratin 34
FRY	−1.62	Furry homolog (Drosophila)
KRTAP14|LOC728952|LOC730743	−1.63	Similar to keratin associated protein 1–1 | hypothetical LOC728952
LOXL4	−1.69	Lysyl oxidase-like 4
STC1	−1.71	Stanniocalcin 1
GBP4	−1.76	Guanylate binding protein 4
RGS4	−1.78	Regulator of G-protein signaling 4
KRTAP1–5|LOC728956	−1.92	Keratin associated protein 1–5 | hypothetical LOC728956
KRTAP1–5|LOC728956	−1.92	Keratin associated protein 1–5 | hypothetical LOC728956
DUSP6	−2.05	Dual specificity phosphatase 6
$hESF_{endo}$ EP48 vs. $hESF_{endo}$ E48		
IMPA2	1.66	Inositol(myo)-1(or 4)-monophosphatase 2
METTL7A	1.56	Methyltransferase like 7A
IL1R1	1.55	Interleukin 1 receptor, type I

[a] Comparison $hESF_{endo}$ EP6 versus $hESF_{endo}$ E6 revealed no significantly regulated genes at 1.5-fold change.

TABLE 5. List of regulated genes (BH corrected P value < 0.05) in comparison of $hESF_{nonendo}$ or $hESF_{endo}$ treated with E_2P_4 for 14 days (EP14) versus $hESF_{nonendo}$ or $hESF_{endo}$ treated with E_2 for 14 days (E14), expressed as fold change (FC).

Gene symbol	FC	Gene description
$hESF_{nonendo}$ EP14 vs. $hESF_{nonendo}$ E14		
SPARCL1	27.49	SPARC-like 1 (mast9, hevin)
ABI3BP	23.24	ABI gene family, member 3 (NESH) binding protein
P2RY14	16.35	Purinergic receptor P2Y, G-protein coupled, 14
IGF1	6.94	Insulin-like growth factor 1 (somatomedin C)
MAOB	6.60	Monoamine oxidase B
FKBP5|LOC285847	6.37	FK506 binding protein 5 | hypothetical protein LOC285847
SLC7A8	5.86	Solute carrier family 7 (cationic amino acid transporter, y+ system), member 8
ENPP1	5.83	Ectonucleotide pyrophosphatase/phosphodiesterase 1
GPX3	5.61	Glutathione peroxidase 3 (plasma)
RORB	5.34	RAR-related orphan receptor B
IMPA2	4.69	Inositol(myo)-1(or 4)-monophosphatase 2
OMD	3.84	Osteomodulin
PRL	3.78	Prolactin
ADRA2C	3.74	Adrenergic, alpha-2C-, receptor
THSD7A	3.67	Thrombospondin, type I, domain containing 7A
NLGN4X	3.66	Neuroligin 4, X-linked
ZBTB16	3.65	Zinc finger and BTB domain containing 16
MYOCD	3.58	Myocardin
CD226	3.53	CD226 molecule
IGFBP1	3.35	Insulin-like growth factor binding protein 1
MAOA	3.32	Monoamine oxidase A
PLXNC1	3.28	Plexin C1
MOBKL2B	3.25	MOB1, Mps One Binder kinase activator-like 2B (yeast)
MUM1L1	3.20	Melanoma associated antigen (mutated) 1-like 1
THBD	3.19	Thrombomodulin
LRIG1	3.12	Leucine-rich repeats and immunoglobulin-like domains 1
SORBS1	2.98	Sorbin and SH3 domain containing 1
INSR	2.95	Insulin receptor
CRISPLD2	2.92	Cysteine-rich secretory protein LCCL domain containing 2
CPM	2.89	Carboxypeptidase M
LCP1	2.83	Lymphocyte cytosolic protein 1 (L-plastin)
SERPINE1	2.82	Serpin peptidase inhibitor, clade E (nexin, plasminogen activator inhibitor type 1), member 1
C10orf10	2.62	Chromosome 10 open reading frame 10
CORIN	2.58	Corin, serine peptidase
UST	2.57	Uronyl-2-sulfotransferase
CNR1	2.55	Cannabinoid receptor 1 (brain)
ADH1B	2.54	Alcohol dehydrogenase 1B (class I), beta polypeptide
IL1R1	2.52	Interleukin 1 receptor, type I
LASS6	2.46	LAG1 homolog, ceramide synthase 6
TNC	2.41	Tenascin C (hexabrachion)
KLF6	2.36	Kruppel-like factor 6
OLFML2B	2.33	Olfactomedin-like 2B
PRLR	2.33	Prolactin receptor
APCDD1	2.26	Adenomatosis polyposis coli down-regulated 1
ERRFI1	2.22	ERBB receptor feedback inhibitor 1
GLB1L2	2.22	Galactosidase, beta 1-like 2
ACSL1	2.19	Acyl-CoA synthetase long-chain family member 1
RHOU	2.19	Ras homolog gene family, member U
PTHLH	2.14	Parathyroid hormone-like hormone
EFHD1	2.14	EF-hand domain family, member D1
SYTL4	2.13	Synaptotagmin-like 4 (granuphilin-a)
TSC22D3	2.11	TSC22 domain family, member 3
TIMP3	2.11	TIMP metallopeptidase inhibitor 3 (Sorsby fundus dystrophy, pseudoinflammatory)
MAP3K4	2.11	Mitogen-activated protein kinase kinase kinase 4
ABCC9	2.08	ATP-binding cassette, sub-family C (CFTR/MRP), member 9
SPSB1	2.04	SplA/ryanodine receptor domain and SOCS box containing 1
ENPEP	2.01	Glutamyl aminopeptidase (aminopeptidase A)
ADCY1	2.00	Adenylate cyclase 1 (brain)
C14orf147	1.98	Chromosome 14 open reading frame 147
APOD	1.97	Apolipoprotein D
IRS2	1.93	Insulin receptor substrate 2
ADAMTS1	1.91	ADAM metallopeptidase with thrombospondin type 1 motif, 1
LHFP	1.91	Lipoma HMGIC fusion partner
ZEB1	1.88	Zinc finger E-box binding homeobox 1
GPRC5B	1.84	G protein-coupled receptor, family C, group 5, member B
SESTD1	1.83	SEC14 and spectrin domains 1
PCBP3	1.82	Poly(rC) binding protein 3
FAM19A2	1.82	Family with sequence similarity 19 (chemokine (C-C motif)-like), member A2
MMD	1.81	Monocyte to macrophage differentiation-associated
DKK1	1.80	Dickkopf homolog 1 (Xenopus laevis)
SLC46A3	1.79	Solute carrier family 46, member 3
COL4A1	1.79	Collagen, type IV, alpha 1

TABLE 5. Continued.

Gene symbol	FC	Gene description
METTL7A	1.79	Methyltransferase like 7A
ACTA2	1.77	Actin, alpha 2, smooth muscle, aorta
FERMT2	1.76	Fermitin family homolog 2 (Drosophila)
ACTG2	1.76	Actin, gamma 2, smooth muscle, enteric
HAND2	1.76	Heart and neural crest derivatives expressed 2
LMOD1	1.75	Leiomodin 1 (smooth muscle)
TMEM37	1.74	Transmembrane protein 37
NBLA00301	1.71	Nbla00301
IRF6	1.70	Interferon regulatory factor 6
CFH	1.70	Complement factor H
SULF2	1.67	Sulfatase 2
CD302	1.66	CD302 molecule
ULK4	1.66	Unc-51-like kinase 4 (C. elegans)
GCNT1	1.65	Glucosaminyl (N-acetyl) transferase 1, core 2 (beta-1,6-N-Acetylglucosaminyltransferase)
ABHD5	1.65	Abhydrolase domain containing 5
MITF	1.64	Microphthalmia-associated transcription factor
PPAP2B	1.64	Phosphatidic acid phosphatase type 2B
CFHR1	1.64	Complement factor H-related 1
ITGA10	1.61	Integrin, alpha 10
AKAP13	1.61	A kinase (PRKA) anchor protein 13
ADH1C	1.60	Alcohol dehydrogenase 1C (class I), gamma polypeptide
ADAMTS2	1.59	ADAM metallopeptidase with thrombospondin type 1 motif, 2
SLC41A2	1.59	Solute carrier family 41, member 2
ID3	1.59	Inhibitor of DNA binding 3, dominant negative helix-loop-helix protein
PRR15	1.58	Proline rich 15
HSD17B11	1.58	Hydroxysteroid (17-beta) dehydrogenase 11
SORT1	1.58	Sortilin 1
JAK2	1.58	Janus kinase 2 (a protein tyrosine kinase)
AVPR1A	1.57	Arginine vasopressin receptor 1A
CHSY3	1.57	Chondroitin sulfate synthase 3
ZCCHC6	1.57	Zinc finger, CCHC domain containing 6
NFIL3	1.57	Nuclear factor, interleukin 3 regulated
EMP2	1.56	Epithelial membrane protein 2
PEMT	1.56	Phosphatidylethanolamine N-methyltransferase
RASL11A	1.55	RAS-like, family 11, member A
ANTXR2	1.55	Anthrax toxin receptor 2
KIAA1217	1.55	KIAA1217
DIAPH2	1.55	Diaphanous homolog 2 (Drosophila)
CHST7	1.55	Carbohydrate (N-acetylglucosamine 6-O) sulfotransferase 7
KCNK6	1.54	Potassium channel, subfamily K, member 6
MTR	1.52	5-Methyltetrahydrofolate-homocysteine methyltransferase
CCDC102B	1.52	Coiled-coil domain containing 102B
KLHL23|PHOSPHO2	1.51	Kelch-like 23 (Drosophila) | phosphatase, orphan 2
ABLIM1	1.51	Actin binding LIM protein 1
ID4	1.51	Inhibitor of DNA binding 4, dominant negative helix-loop-helix protein
PHF17	1.51	PHD finger protein 17
FOXO1	1.50	Forkhead box O1
TMED8	1.50	Transmembrane emp24 protein transport domain containing 8
TLR4	1.50	Toll-like receptor 4
GREB1	1.50	Growth regulation by estrogen in breast cancer 1
C2orf59|LOC541471	−1.50	Chromosome 2 open reading frame 59 | hypothetical LOC541471
GREM1	−1.51	Gremlin 1, cysteine knot superfamily, homolog (Xenopus laevis)
SYT16	−1.52	Synaptotagmin XVI
FLJ36031	−1.52	Hypothetical protein FLJ36031
IFIT1	−1.53	Interferon-induced protein with tetratricopeptide repeats 1
ARHGAP18	−1.54	Rho GTPase activating protein 18
ETV5	−1.54	Ets variant gene 5 (ets-related molecule)
SNRK	−1.54	SNF related kinase
LOXL4	−1.55	Lysyl oxidase-like 4
LIMA1	−1.55	LIM domain and actin binding 1
CYFIP2	−1.56	Cytoplasmic FMR1 interacting protein 2
INPP4B	−1.57	Inositol polyphosphate-4-phosphatase, type II, 105kDa
C6orf138	−1.58	Chromosome 6 open reading frame 138
IL13RA2	−1.58	Interleukin 13 receptor, alpha 2
CCND1	−1.60	Cyclin D1
NAV3	−1.61	Neuron navigator 3
ISOC1	−1.61	Isochorismatase domain containing 1
SAMD12	−1.62	Sterile alpha motif domain containing 12
HSPC159	−1.64	Galectin-related protein
BDKRB1	−1.64	Bradykinin receptor B1
NT5E	−1.65	5′-Nucleotidase, ecto (CD73)
MYO1B	−1.67	Myosin IB
SERPINB2	−1.67	Serpin peptidase inhibitor, clade B (ovalbumin), member 2

TABLE 5. Continued.

Gene symbol	FC	Gene description
SDC4	−1.68	Syndecan 4
SMAD3	−1.69	SMAD family member 3
HERC5	−1.69	Hect domain and RLD 5
PLCB1	−1.69	Phospholipase C, beta 1 (phosphoinositide-specific)
IGFBP6	−1.70	Insulin-like growth factor binding protein 6
AFAP1L2	−1.75	Actin filament associated protein 1-like 2
FAM43A	−1.76	Family with sequence similarity 43, member A
RAB3B	−1.83	RAB3B, member RAS oncogene family
KRTAP1–4|LOC728952|LOC730743	−1.83	Similar to keratin associated protein 1–1 | hypothetical LOC728952
ST8SIA1	−1.86	ST8 alpha-N-acetyl-neuraminide alpha-2,8-sialyltransferase 1
RGS4	−1.87	Regulator of G-protein signaling 4
PTN	−1.89	Pleiotrophin (heparin binding growth factor 8, neurite growth-promoting factor 1)
ARL4C	−1.90	ADP-ribosylation factor-like 4C
FJX1	−1.97	Four jointed box 1 (Drosophila)
NEFM	−1.97	Neurofilament, medium polypeptide 150kDa
FHOD3	−2.03	Formin homology 2 domain containing 3
ATP8B1	−2.05	ATPase, class I, type 8B, member 1
F2RL2	−2.12	Coagulation factor II (thrombin) receptor-like 2
IGFBP5	−2.15	Insulin-like growth factor binding protein 5
KRT34	−2.17	Keratin 34
DUSP6	−2.18	Dual specificity phosphatase 6
C4orf31	−2.20	Chromosome 4 open reading frame 31
PROM1	−2.23	Prominin 1
STC1	−2.29	Stanniocalcin 1
CCRL1	−2.52	Chemokine (C-C motif) receptor-like 1
GBP4	−2.54	Guanylate binding protein 4
KRTAP1–5|LOC728956	−2.67	Keratin associated protein 1–5 | hypothetical LOC728956
$hESF_{endo}$ EP14 vs. $hESF_{endo}$ E14		
C10orf10	1.66	Chromosome 10 open reading frame 10
SLC7A8	1.61	Solute carrier family 7 (cationic amino acid transporter, y+ system), member 8
ADH1B	1.60	Alcohol dehydrogenase 1B (class I), beta polypeptide
IL1R1	1.59	Interleukin 1 receptor, type I

Tables 3–5 and Supplemental Tables S1–S3). Significantly regulated canonical pathways and network formations in response to E_2P_4 versus that of E_2 treatment in $hESF_{nonendo}$ and $hESF_{endo}$ and in $hESF_{endo}$ versus $hESF_{nonendo}$ are shown in Supplemental Tables S4 and S5.

Canonical pathways. Canonical pathways regulated at early and intermediate time points in the $hESF_{nonendo}$ response to E_2P_4 versus E_2 treatment were related to lipid and carbohydrate metabolism, *O*-glycan biosynthesis, neuregulin, and cAMP signaling. At 14 days, there was activation of the IGF1 signaling and integrin-linked kinase (ILK) pathways and activation by the VDR/RXR and hepatic fibrosis pathways. In contrast, the $hESF_{endo}$ response to E_2P_4 versus E_2 treatment was blunted, with fewer genes being regulated and subsequently being involved in canonical pathways. Moreover, pathways activated in $hESF_{endo}$ differed from those activated in $hESF_{nonendo}$ in response to E_2P_4 versus E_2 treatment. Differences were observed in interleukin (IL)10 and IL6 signaling pathways, PPAR signaling, LXR/RXR activation, and bile acid and glucose biosynthesis and metabolism pathways in early and late responses to E_2P_4 versus E_2 treatment (Supplemental Table S4).

Networks. Network analysis of genes upregulated in the early (6-h) response to E_2P_4 versus E_2 treatment in $hESF_{nonendo}$ revealed enrichment of biological processes involving carbohydrate, lipid, and amino acid metabolism and tissue morphology. In contrast, in the (48-h) intermediate response, disease and development-associated networks prevailed, including cancer, cardiovascular, and gastrointestinal disease, tissue development, cell morphology, and embryonic development. The late response of $hESF_{nonendo}$ at 14 days showed involvement of networks including DNA replication, recombination, and repair, nucleic acid metabolism, skeletal and muscular system development and function, endocrine system disorders, and gene expression. IPA analysis of the $hESF_{endo}$ early response involved tissue developmental processes (nervous system, skeletal, muscular, connective tissue, and hematologic) and cell–cell signaling and cell cycle. The intermediate response revealed the formation of cancer, cell death, neurological disease, posttranslational modification, cell cycle, cellular development, and cell signaling networks, which differs from the $hESF_{nonendo}$ response at this time point. Differences between $hESF_{endo}$ and $hESF_{nonendo}$ at 14 days of treatment revealed networks involving cancer, cell growth and proliferation, cell–cell signaling, cell movement, nucleic acids, drugs, and lipid metabolism (Supplemental Table S5).

DISCUSSION

General Comments

This study reveals for the first time the kinetic expressions of specific genes, pathways, and networks during early, intermediate, and late responses to P_4 (E_2P_4 vs. E_2) in hESF from women with and without endometriosis. In this in vitro model, there are likely a multiplicity of pathways and processes that are initiated and perhaps synergistically affected by E_2P_4 treatment and separately by E_2 treatment, although the response to E_2 was significantly limited to *PGR* upregulation at all time points, supporting the data obtained herein as likely to be P_4-mediated events. Nonetheless, there may be other responses that are not strictly P_4-mediated in our model; however, identifying the classically P_4-regulated genes was consistent with the effectiveness of a functional P_4 pathway in $hESF_{nonendo}$ and a dysfunctional pathway in $hESF_{endo}$.

In $hESF_{nonendo}$, distinct biological and molecular processes and signaling pathways were observed; whereas, signaling

pathways in the $hESF_{endo}$ responses to E_2P_4 versus E_2 treatment were not active compared to those in $hESF_{nonendo}$, due to the limited number of genes regulated. A blunted $hESF_{endo}$ response to P_4 was observed, with limited expression of many P_4-regulated genes and curtailed activation of distinct canonical pathways and processes. While the *PGRB*/*PGRA* ratio was reported to be lower in endometrial tissues from women with endometriosis than in tissues from healthy volunteers [15], our earlier studies of eutopic endometrium did not confirm significant differences in *PGR* isoforms in either tissue biopsies or hESF from women with endometriosis versus those without endometriosis [10]. In the present study, we hypothesized and have found that the P_4 resistance in eutopic endometrium from women with endometriosis results not from the *PGR* aberrant expression but rather from its delayed upregulation in the early response to E_2. Moreover, in the current study, the PGR FKBP5 (immunophilin) chaperone expression level, which was upregulated in $hESF_{nonendo}$ in early, intermediate, and late responses to P_4, was not regulated in $hESF_{endo}$ and was significantly lower in $hESF_{endo}$ than in $hESF_{nonendo}$ at $t = 0$. Interestingly, diminished FKBP4 expression has been observed in eutopic and ectopic endometrium in humans and baboons with endometriosis [27, 28]. Furthermore, *Fkbp4*-null mice are prone to develop endometriotic lesions upon inoculation with endometrial tissue [28]. Overall, PGR chaperones (and coregulators [10]) appear to play a role in the blunted response of hESF to P_4 in women with endometriosis.

We propose that the normal response of hESF to P_4 (E_2P_4 vs. E_2) involves a tightly regulated kinetic cascade involving key components in the PGR and MAPK signaling pathways that results in inhibition of E_2-mediated proliferation, establishment of key networks, and eventual differentiation to the decidual phenotype. Furthermore, we propose that these early events, which are likely temporal and spatial in nature, are not established in the early $hESF_{endo}$ response to P_4, contributing to abnormal P_4 responsiveness of this cell type in eutopic endometrium of women with endometriosis. A similar mechanism may be ongoing in ectopic foci.

Our earlier studies using eutopic endometrial tissue samples from women with and without endometriosis [25, 26] revealed dysregulation of a number of P_4-responsive genes and signaling molecules. In those earlier studies we specifically validated the dysregulation of the primarily stromal fibroblast (hESF) products ERRFI1, FOXO1A, CDC2, IGFBP1, PRL, GPX3, and DKK1 in endometrial tissue from women with disease [25, 26]. Many of these gene products were found to be similarly dysregulated in our current in vitro study of hESF, and thus, essentially their in vivo expression has been validated by our previous work.

$hESF_{nonendo}$ Response to Progesterone

Early and intermediate responses. The first observable response to P_4 in vivo occurs in early secretory endometrium and includes P_4 inhibition of E_2-induced cellular proliferation and an increase in cholesterol, fatty acid, prostaglandin, glycogen, and transporter biosynthesis, mostly in epithelium, with little known about the early hESF response [8]. In mid-secretory endometrium, hESF begin to make a transition from a fibroblast-like spindle to a rounder morphology and a secretory phenotype, typical of epithelium, producing classical ''decidual markers'' (e.g., prolactin and IGFBP1). In vitro, hESF respond to P_4 (plus E_2), P_4 plus cAMP, or only cAMP, with characteristic morphologic and gene expression and protein changes, as in vivo. Treating cells with cAMP or P_4 plus cAMP results in upregulation of decidual markers within 48–72 h, compared to 8–14 days (as in vivo [12]), with P_4 treatment alone. Direct transcriptional control by P_4 has been questioned due to the time course in vivo [12], and P_4 has been proposed to maintain the decidual response initiated by a yet-to-be identified ligand stimulating the PKA pathway [12]. The data herein support an early response to P_4 that includes unique early response genes and intracellular signaling pathways and subsequent expression of decidual markers involving stimulation of the PKA pathway.

What is striking in the early $hESF_{nonendo}$ response to P_4 is EGFR-mediated and MAPK signaling. The ERBB receptor feedback inhibitor 1 (*ERRFI1*, or mitogen-inducible gene 6 [*MIG6*]) is a negative regulator of EGFR-mediated mitogenic signaling [29] and is one of the earliest transcription factors upregulated in P_4-treated hESF. The protein regulates the duration of MAPK activation via attenuation of *EGFR* autophosphorylation in a mouse knockout model [29]. Our data support P_4 regulation of this signaling pathway early in the P_4 response in $hESF_{nonendo}$.

Other early and intermediate response genes upregulated in the $hESF_{nonendo}$ response to P_4 (E_2P_4 vs. E_2) are the *DKK1* gene of the Wnt family, the solute carrier family SLC7A8 and IMPA2 proteins, and, interestingly, the adrenergic receptor alpha-2C (*ADRA2C*) gene; this last gene is one of several neuronal receptors found in endometrium [24, 30]. Expression of the *ADRA2C* transcript in P_4-treated $hESF_{nonendo}$ suggests that normal endometrium possesses the machinery for regulating neurotransmission [31]. Marked *IMPA2* upregulation underscores the importance of the phosphatidylinositol signaling pathway [32] in the response of hESF to P_4.

The SPARCL1 protein (a SPARC-like 1 [hevin], or mast9, or high endothelial venule protein), an extracellular matrix-associated protein member of the SPARC family, is upregulated during the implantation window and is associated with the E_2P_4 versus the E_2 response of cultured explants from late proliferative phase human endometrium [33]. It is expressed in many tissues and is associated with collagen fibrils [34]. *SPARCL1* expression is downregulated in several tumors and negatively regulates cell cycle progression, cell proliferation, and migration [35, 36]. In the present study, *SPARCL1* expression was highly upregulated in response to P_4 in $hESF_{nonendo}$ at 6 and 48 h and 14 days, suggesting a major role for the protein product in the P_4 response of hESF, perhaps participating in or directly inhibiting cell cycle progression and enabling differentiation in response to P_4.

Late response. At 14 days, genes corresponding to secretory and cell adhesion proteins, including classical decidual markers, as well as interleukins, signaling components, enzymes, and receptors, are upregulated (Table 5), with the *SPARCL1* gene mentioned above being the most highly upregulated gene. Also of interest is the *CNR1* cannabinoid receptor, shown recently to be expressed in human endometrium throughout the cycle, without significant cyclic variations [37]. Although P_4 has been shown to activate the endocannabinoid-degrading enzyme fatty acid amide hydrolase in human lymphocytes [38], this is the first study of P_4 regulation of the endocannabinoid system in human endometrium. The significance of *CNR1* expression in hESF warrants further investigation.

One of the most highly upregulated genes, *ENPP1*, regulates extracellular pyrophosphate, a major inhibitor of extracellular matrix (ECM) calcification [39]. Also, by Day 14, many known P_4-regulated genes are increased, and several genes associated with actin filaments and bundle formation are up- or downregulated (Table 5), consistent with changes in cell

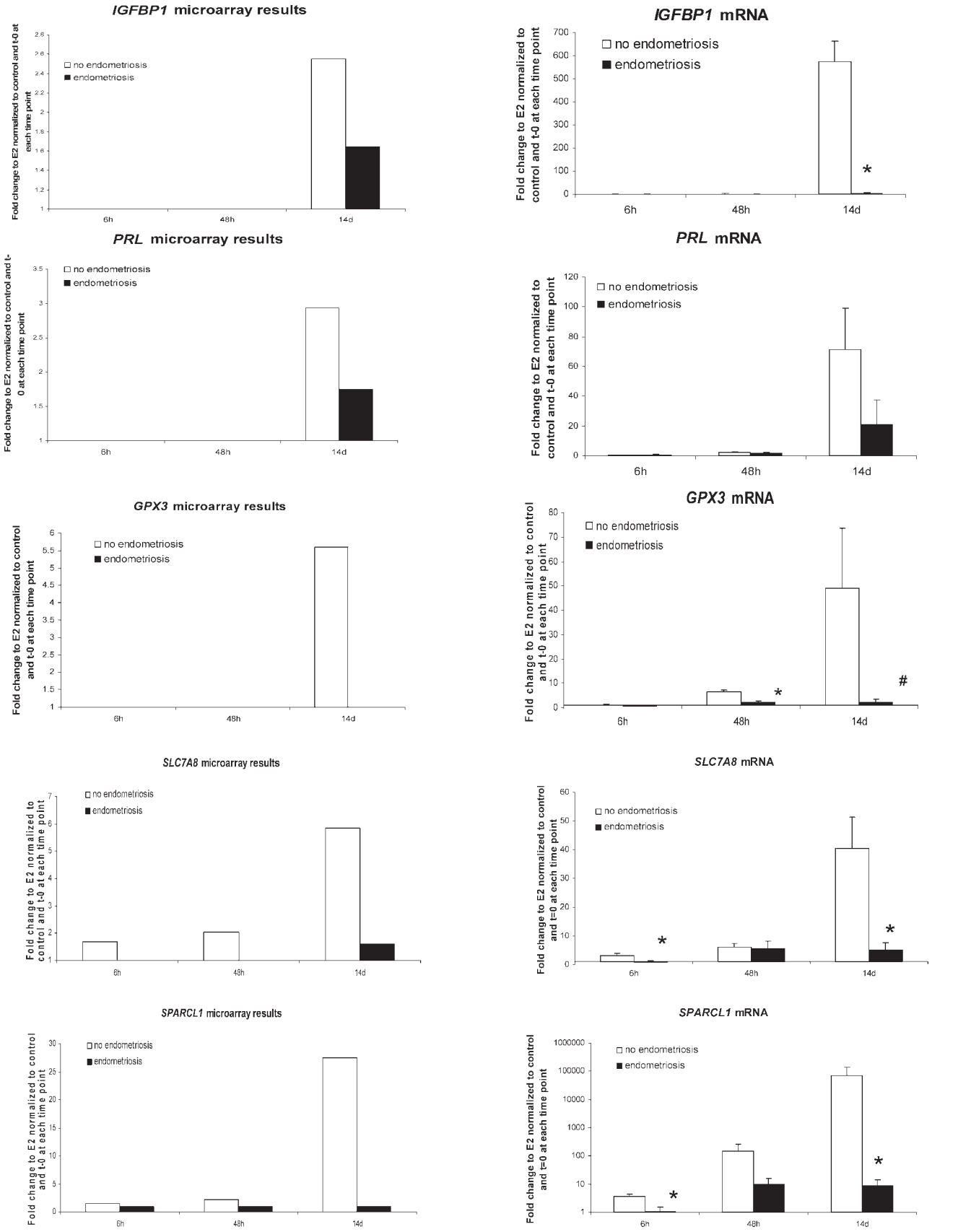

FIG. 3. Validation of microarray gene expression profiling by QRT-PCR. **Right column** indicates fold change expression of genes in the microarray data set in the present study. **Left column** indicates QRT-PCR validation of microarray data of gene expression in $hESF_{nonendo}$ and $hESF_{endo}$ treated with or without E_2 and P_4 for 6 h, 48 h, and 14 days (n = 4 in each group). Y axis displays the fold change of expression in hESF treated withP_4 and E_2, relative to E_2 and normalized to the vehicle control and $t = 0$ at each time point. *, Significance accepted at $P \leq 0.05$. #, Significance accepted at $P = 0.05$. Error bars represent means ± SEM.

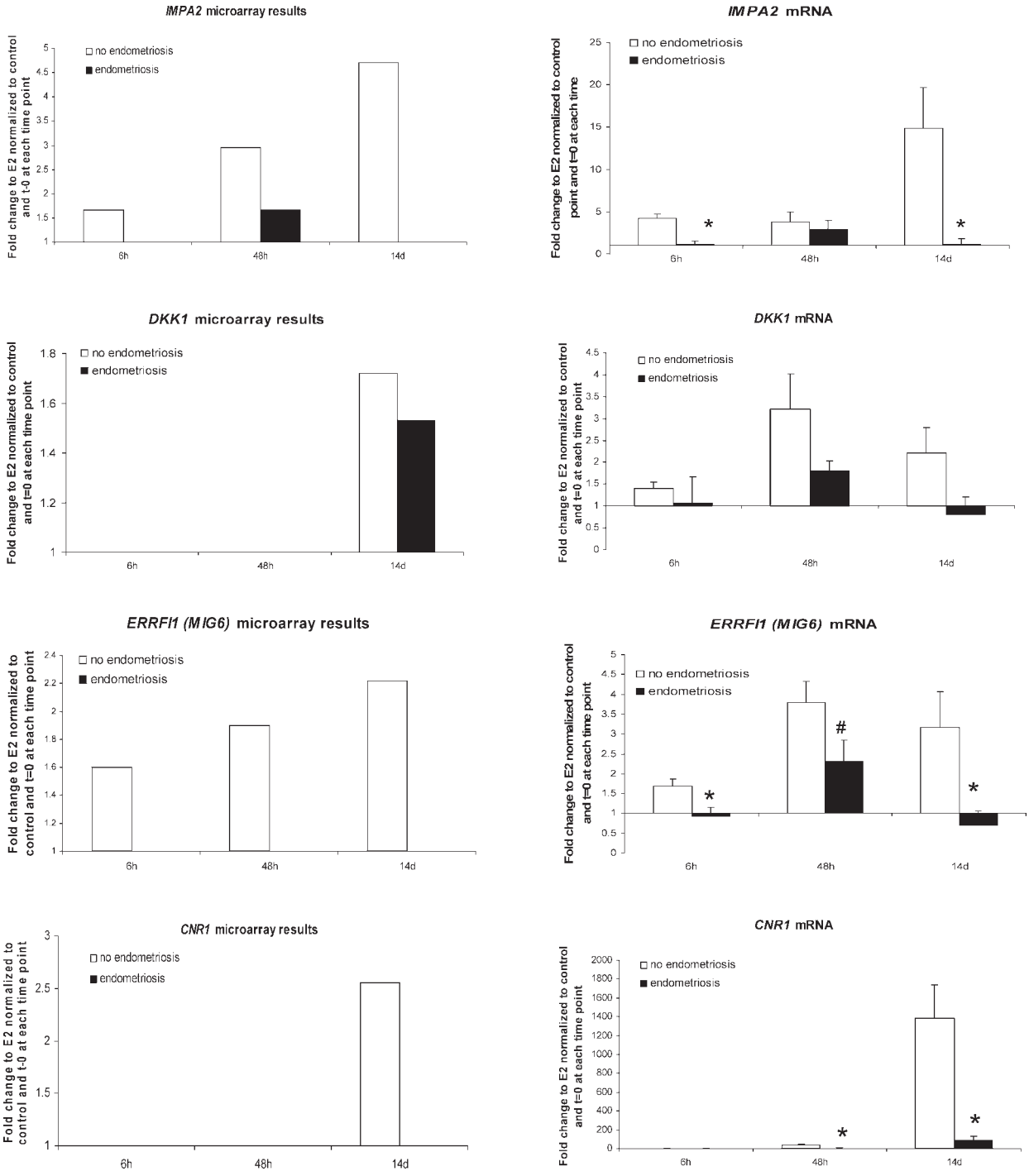

FIG. 3. Continued.

shape in the late response to P_4. Thus, the gene expression profile at Day 14 represents classically decidualizing hESF, based on the cytoskeletal and stress fiber changes, the secretory phenotype, and a predominance of genes involved in the ECM, cell matrix, and cell–cell communication.

Several groups have investigated the transcriptome of decidualized human hESF (summarized in Supplemental Table S6). The current study compared hESF treated with E_2P_4 versus E_2 and showed a time course of this comparison, focusing on early, intermediate, and late responses to P_4, per se, of hESF (both $hESF_{nonendo}$ and $hESF_{endo}$). Okada and colleagues [40] analyzed genes expressed in $hESF_{nonendo}$ after 3 days of P_4 treatment (without E_2) using a 1000-gene cDNA platform and found 6 genes were upregulated and 27 genes were downregulated by P_4, compared to controls (vehicle alone). Among those downregulated was the *IGFBP5* gene and pregnancy-specific glycoproteins, and among those upregulated was the *IL1RI* gene, as also found herein. The differences observed between the two studies were probably due to different treatment protocols (e.g., no priming with E_2), duration of hormonal treatments, and use of different array platforms.

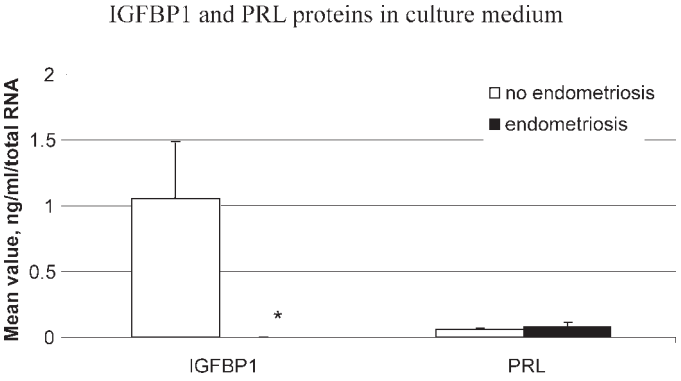

FIG. 4. Validation of microarray gene expression profiling by ELISA. IGFBP1 and PRL protein secretion in CM from $hESF_{nonendo}$ and $hESF_{endo}$ treated with or without E_2 and P_4 for 14 days (n = 4 in each group), normalized to the total RNA level. *, Significance accepted at $P \leq 0.05$. Error bars represent means ± SEM.

$hESF_{endo}$ Response to Progesterone

Early, intermediate, and late responses. There were significantly lower numbers of genes regulated by P_4 (E_2P_4 vs. E_2) in $hESF_{endo}$ versus $hESF_{nonendo}$ (Tables 4, 5). In women with endometriosis, in contrast to those without disease, ERRFI1 is not upregulated in secretory phase tissue [25, 41], further supporting its regulation by P_4 and dysregulation in this P_4-resistant disorder, confirmed herein on the cellular level. We have previously shown that increased activation of MAPK1/3 in $hESF_{endo}$ contributes to persistent proliferative changes in secretory-phase endometrium in women with endometriosis [41]. Constitutive expression of the AREG and HBEGF EGFR ligands in $hESF_{endo}$ that can activate MAPK1/3 [42–44], and were observed herein, provides a potential mechanism for the observed constitutive MAPK1/3 phosphorylation and the proliferative phenotype of $hESF_{endo}$. This may play an important role in the pathophysiology of the disease and design of targeted therapies for endometriosis and is under study in our laboratory.

We previously analyzed transcriptomes of hESF (both $hESF_{nonendo}$ and $hESF_{endo}$) in response to 8-Br-cAMP for 96 h (full decidualization phenotype) [9]. A comparison of lists of genes of decidualized $hESF_{nonendo}$ in response to P_4 (14 days) versus those of 8-Br-cAMP (96 h) revealed 30 common genes, among them *PRL*, *IGFBP1*, *ADRA2C*, *CCND1*, *IL1R1*, and stanniocalcin (Supplemental Table S7), reflecting the decidualization signature of $hESF_{nonendo}$. Of note, no common genes were found when similar comparisons were performed with $hESF_{endo}$ (Supplemental Table S7).

Herein, the (*CCND1*) cyclin D1 transcript was increased in $hESF_{endo}$ versus $hESF_{nonendo}$ treated with E_2P_4 for 14 days, while it was decreased in $hESF_{nonendo}$ in response to P_4 (E_2P_4 vs. E_2). This confirms our previous results showing an increased proliferative potential with increased *CCND1* expression in decidualized $hESF_{endo}$ versus $hESF_{nonendo}$ and a blunted response of $hESF_{endo}$ to cAMP (decreased PKA activation in $hESF_{endo}$ here) [9, 41].

In contrast to the upregulation of the *SPARCL1* gene in response to P_4 in $hESF_{nonendo}$, *SPARCL1* expression was not regulated by P_4 in $hESF_{endo}$. Importantly, it was the most downregulated gene in $hESF_{endo}$ versus $hESF_{nonendo}$, underscoring the decreased responsiveness of $hESF_{endo}$ to P_4 treatment. As *SPARCL1* expression is an inhibitor of cell proliferation, its upregulation in decidualized $hESF_{nonendo}$ and downregulation in $hESF_{endo}$ suggest a role for it in the proliferative phenotype of $hESF_{endo}$.

Interestingly, cancer-associated signaling pathways, such as those in colorectal cancer metastasis and bladder cancer signaling, were regulated in $hESF_{endo}$ versus $hESF_{nonendo}$ (Supplemental Table S4). Regulation of these canonical pathways in $hESF_{endo}$ is consistent with the invasive phenotype of endometriosis that may be shared by other invasive cell types and tissues.

Among several signaling pathways that were significantly dysregulated in the $hESF_{endo}$ response to P_4, versus that of $hESF_{nonendo}$ (Supplemental Table S4), are those involving axonal guidance and neuropathic pain signaling ($P = 0.0048$ and $P = 0.01$, respectively) (Supplemental Table S4). Adrenergic and sensory nerve fibers have recently been described in eutopic endometrium of women with endometriosis (but not in women without endometriosis) [45], which may contribute to pain associated with the disorder. Thus, it is of particular interest that in the $hESF_{nonendo}$ response to P_4 (E_2P_4 vs. E_2), there is sustained *ADRA2C* upregulation and downregulation of neurofilament medium polypeptide (*NEFM*) and pleiotrophin (heparin-binding growth factor 8, neurite growth-promoting factor 1). Pleiotrophin, associated with angiogenesis and neurite growth, is expressed in normal endometrium throughout the menstrual cycle and is significantly upregulated in endometrium from women with advanced-stage endometriosis [46]. The molecular mechanisms underlying the presence of nerve fibers within eutopic endometrium of women with endometriosis are not well understood; however, the data herein support a role for hESF in promoting neurite growth and axonal guidance within the endometrium of women with endometriosis and, potentially, hormonal regulation of nerve fibers and nerve bundle density in this tissue from women with disease [47]. We are currently investigating this in our laboratory.

The current study has given unique insight into the genome-wide transcriptome of the human endometrial stromal fibroblast at early, intermediate, and late responses to P_4, in an experimental paradigm that reveals kinetic changes in gene expression, biological processes, and signaling pathways. Some of these changes are novel and some are consistent with known hESF responses to P_4 in vivo and resistance to P_4 actions and dysregulation in disorders such as endometriosis. The signaling pathways described herein may serve as unique targets for drugs to treat endometrial disorders.

REFERENCES

1. Cramer DW, Missmer SA. The epidemiology of endometriosis. Ann N Y Acad Sci 2002; 955:11–22.
2. Eskenazi B, Warner ML. Epidemiology of endometriosis. Obstet Gynecol Clin NorthAm 1997; 24:235–258.
3. Giudice LC. Clinical practice. Endometriosis. N Engl J Med 2010; 362: 2389–2398.
4. Aghajanova L, Velarde MC, Giudice LC. Altered gene expression profiling in endometrium: evidence for progesterone resistance. Semin Reprod Med 2010; 28:51–58.
5. Bulun SE. Endometriosis. N Engl J Med 2009; 360:268–279.
6. Giudice LC. Endometrium in PCOS: Implantation and predisposition to endocrine CA. Best Pract Res Clin Endocrinol Metab 2006; 20:235–244.
7. Irwin JC, Giudice LC. The decidua. In: Knobil E, Neill JD (eds.), Encyclopedia of Reproduction. San Diego: Aademic Press; 1998:823–835.
8. Giudice LC. Application of functional genomics to primate endometrium: insights into biological processes. Reprod Biol Endocrinol 2006; 4(suppl 1):S4.
9. Aghajanova L, Horcajadas JA, Weeks JL, Esteban FJ, Nezhat CN, Conti M, Giudice LC. The protein kinase A pathway-regulated transcriptome of endometrial stromal fibroblasts reveals compromised differentiation and persistent proliferative potential in endometriosis. Endocrinology 2010; 151:1341–1355.
10. Aghajanova L, Velarde MC, Giudice LC. The progesterone receptor

coactivator Hic-5 is involved in the pathophysiology of endometriosis. Endocrinology 2009; 150:3863–3870.
11. Brar AK, Frank GR, Kessler CA, Cedars MI, Handwerger S. Progesterone-dependent decidualization of the human endometrium is mediated by cAMP. Endocrine 1997; 6:301–307.
12. Gellersen B, Brosens J. Cyclic AMP and progesterone receptor cross-talk in human endometrium: a decidualizing affair. J Endocrinol 2003; 178: 357–372.
13. Jones MC, Fusi L, Higham JH, Abdel-Hafiz H, Horwitz KB, Lam EW, Brosens JJ. Regulation of the SUMO pathway sensitizes differentiating human endometrial stromal cells to progesterone. Proc Natl Acad Sci U S A 2006; 103:16272–16277.
14. Attia GR, Zeitoun K, Edwards D, Johns A, Carr BR, Bulun SE. Progesterone receptor isoform A but not B is expressed in endometriosis. J Clin Endocrinol Metab 2000; 85:2897–2902.
15. Igarashi TM, Bruner-Tran KL, Yeaman GR, Lessey BA, Edwards DP, Eisenberg E, Osteen KG. Reduced expression of progesterone receptor-B in the endometrium of women withendometriosis and in cocultures of endometrial cells exposed to 2,3,7,8-tetrachlorodibenzo-p-dioxin. Fertil Steril 2005; 84:67–74.
16. Xue Q, Lin Z, Cheng YH, Huang CC, Marsh E, Yin P, Milad MP, Confino E, Reierstad S, Innes J, Bulun SE. Promoter methylation regulates estrogen receptor 2 in human endometrium and endometriosis. Biol Reprod 2007; 77:681–687.
17. Xue Q, Lin Z, Yin P, Milad MP, Cheng YH, Confino E, Reierstad S, Bulun SE. Transcriptional activation of steroidogenic factor-1 by hypomethylation of the 5′ CpG island in endometriosis. J Clin Endocrinol Metab 2007; 92:3261–3267.
18. Bulun SE, Utsunomiya H, Lin Z, Yin P, Cheng YH, Pavone ME, Tokunaga H, Trukhacheva E, Attar E, Gurates B, Milad MP, Confino E, et al. Steroidogenic factor-1 and endometriosis. Mol Cell Endocrinol 2009; 300:104–108.
19. Klemmt PA, Carver JG, Kennedy SH, Koninckx PR, Mardon HJ. Stromal cells from endometriotic lesions and endometrium from women with-endometriosis have reduced decidualization capacity. Fertil Steril 2006; 85:564–572.
20. Kim JJ, Taylor HS, Lu Z, Ladhani O, Hastings JM, Jackson KS, Wu Y, Guo SW, Fazleabas AT. Altered expression of HOXA10 in endometriosis: potential role in decidualization. Mol Hum Reprod 2007; 13:323–332.
21. Revised American Fertility Society classification of endometriosis. Fertil Steril 1985; 43:351–352.
22. Aghajanova L, Hamilton A, Kwintkiewicz J, Vo KC, Giudice LC. Steroidogenic enzyme and key decidualization marker dysregulation in endometrial stromal cells from women withversus without endometriosis. Biol Reprod 2009; 80:105–114.
23. Tulac S, Overgaard MT, Hamilton AE, Jumbe NL, Suchanek E, Giudice LC. Dickkopf-1, an inhibitor of Wnt signaling, is regulated by progesterone in human endometrial stromal cells. J Clin Endocrinol Metab 2006; 91:1453–1461.
24. Talbi S, Hamilton AE, Vo KC, Tulac S, Overgaard MT, Dosiou C, Le Shay N, Nezhat CN, Kempson R, Lessey BA, Nayak NR, Giudice LC. Molecular phenotyping of human endometrium distinguishes menstrual cycle phases and underlying biological processes in normo-ovulatory women. Endocrinology 2006; 147:1097–1121.
25. Burney RO, Talbi S, Hamilton AE, Vo KC, Nyegaard M, Nezhat CR, Lessey BA, Giudice LC. Gene expression analysis of endometrium reveals progesterone resistance and candidate susceptibility genes in women withendometriosis. Endocrinology 2007; 148:3814–3826.
26. Kao LC, Germeyer A, Tulac S, Lobo S, Yang JP, Taylor RN, Osteen K, Lessey BA, Giudice LC. Expression profiling of endometrium from women withendometriosis reveals candidate genes for disease-based implantation failure and infertility. Endocrinology 2003; 144:2870–2881.
27. Jackson KS, Brudney A, Hastings JM, Mavrogianis PA, Kim JJ, Fazleabas AT. The altered distribution of the steroid hormone receptors and the chaperone immunophilin FKBP52 in a baboon model of endometriosis is associated withprogesterone resistance during the window of uterine receptivity. Reprod Sci 2007; 14:137–150.
28. Hirota Y, Tranguch S, Daikoku T, Hasegawa A, Osuga Y, Taketani Y, Dey SK. Deficiency of immunophilin FKBP52 promotes endometriosis. Am J Pathol 2008; 173:1747–1757.
29. Ferby I, Reschke M, Kudlacek O, Knyazev P, Pante G, Amann K, Sommergruber W, Kraut N, Ullrich A, Fassler R, Klein R. Mig6 is a negative regulator of EGF receptor-mediated skin morphogenesis and tumor formation. Nat Med 2006; 12:568–573.
30. Popovici RM, Kao LC, Giudice LC. Discovery of new inducible genes in in vitro decidualized human endometrial stromal cells using microarray technology. Endocrinology 2000; 141:3510–3513.
31. Kohli U, Muszkat M, Sofowora GG, Harris PA, Friedman EA, Dupont WD, Scheinin M, Wood AJ, Stein CM, Kurnik D. Effects of variation in the human alpha2A- and alpha2C-adrenoceptor genes on cognitive tasks and pain perception. Eur J Pain 2010; 14:154–159.
32. Yoshikawa T, Turner G, Esterling LE, Sanders AR, Detera-Wadleigh SD. A novel human myo-inositol monophosphatase gene, IMP.18p, maps to a susceptibility region for bipolar disorder. Mol Psychiatry 1997; 2:393–397.
33. Dassen H, Punyadeera C, Kamps R, Klomp J, Dunselman G, Dijcks F, de Goeij A, Ederveen A, Groothuis P. Progesterone regulation of implantation-related genes: new insights into the role of oestrogen. Cell Mol Life Sci 2007; 64:1009–1032.
34. Hambrock HO, Nitsche DP, Hansen U, Bruckner P, Paulsson M, Maurer P, Hartmann U. SC1/hevin. An extracellular calcium-modulated protein that binds collagen I. J Biol Chem 2003; 278:11351–11358.
35. Sullivan MM, Puolakkainen PA, Barker TH, Funk SE, Sage EH. Altered tissue repair in hevin-null mice: inhibition of fibroblast migration by a matricellular SPARC homolog. Wound Repair Regen 2008; 16:310–319.
36. Claeskens A, Ongenae N, Neefs JM, Cheyns P, Kaijen P, Cools M, Kutoh E. Hevin is downregulated in many cancers and is a negative regulator of cell growthand proliferation. Br J Cancer 2000; 82:1123–1130.
37. Taylor AH, Abbas MS, Habiba MA, Konje JC. Histomorphometric evaluation of cannabinoid receptor and anandamide modulating enzyme expression in the human endometrium throughthe menstrual cycle. Histochem Cell Biol 2010; 133:557–565.
38. Maccarrone M, Bari M, Di Rienzo M, Finazzi-Agro A, Rossi A. Progesterone activates fatty acid amide hydrolase (FAAH) promoter in human T lymphocytes throughthe transcription factor Ikaros. Evidence for a synergistic effect of leptin. J Biol Chem 2003; 278:32726–32732.
39. Levy-Litan V, Hershkovitz E, Avizov L, Leventhal N, Bercovich D, Chalifa-Caspi V, Manor E, Buriakovsky S, Hadad Y, Goding J, Parvari R. Autosomal-recessive hypophosphatemic rickets is associated withan inactivation mutation in the ENPP1 gene. Am J Hum Genet 2010; 86: 273–278.
40. Okada H, Nakajima T, Yoshimura T, Yasuda K, Kanzaki H. Microarray analysis of genes controlled by progesterone in human endometrial stromal cells in vitro. Gynecol Endocrinol 2003; 17:271–280.
41. Velarde MC, Aghajanova L, Nezhat CR, Giudice LC. Increased mitogen-activated protein kinase kinase/extracellularly regulated kinase activity in human endometrial stromal fibroblasts of women withendometriosis reduces 3′,5′-cyclic adenosine 5′-monophosphate inhibition of cyclin D1. Endocrinology 2009; 150:4701–4712.
42. Gooz M, Gooz P, Luttrell LM, Raymond JR. 5-HT2A receptor induces ERK phosphorylation and proliferation throughADAM-17 tumor necrosis factor-alpha-converting enzyme (TACE) activation and heparin-bound epidermal growthfactor-like growthfactor (HB-EGF) shedding in mesangial cells. J Biol Chem 2006; 281:21004–21012.
43. Jessmon P, Kilburn BA, Romero R, Leach RE, Armant DR. Function-specific intracellular signaling pathways downstream of heparin-binding EGF-like growthfactor utilized by human trophoblasts. Biol Reprod 2010; 82:921–929.
44. Shin HS, Lee HJ, Nishida M, Lee MS, Tamura R, Yamashita S, Matsuzawa Y, Lee IK, Koh GY. Betacellulin and amphiregulin induce upregulation of cyclin D1 and DNA synthesis activity throughdifferential signaling pathways in vascular smoothmuscle cells. Circ Res 2003; 93: 302–310.
45. Tokushige N, Markham R, Russell P, Fraser IS. Different types of small nerve fibers in eutopic endometrium and myometrium in women withendometriosis. Fertil Steril 2007; 88:795–803.
46. Chung J, Uchida E, Grammer TC, Blenis J. STAT3 serine phosphorylation by ERK-dependent and -independent pathways negatively modulates its tyrosine phosphorylation. Mol Cell Biol 1997; 17:6508–6516.
47. Medina MG, Lebovic DI. Endometriosis-associated nerve fibers and pain. Acta Obstet Gynecol Scand 2009; 88:968–975.